Supplementary Information (SI) for Journal of Materials Chemistry A.
This journal is © The Royal Society of Chemistry 2026

Supporting Information

Selective Oxidation of Methanol into Value-Added Chemical over Alkali Etched Silver Nanowires-Ni-ZIF Composite

Jian Lin,[a] Xiao Lian [a] and Helin Niu*[a]

a Anhui Province Key Laboratory of Chemistry for Hybrid Functional Materials, School of Chemistry & Chemical Engineering, Anhui University, Hefei 230601, China; Email: niuhelin@ahu.edu.cn.

Table of Contents

Experimental section

Preparation of Ni-ZIF nanosheet array:

To a solution of nickel nitrate hexahydrate ($Ni(NO_3)_2 \cdot 6H_2O$, 0.25 mmol) and 2-methylimidazole (2-Melm) (1 mmol) in a mixed solvent of methanol and ethanol (25 mL, V:V = 4:1). The system was transferred into a 50 mL round-bottomed flask and stirred in an oil bath at 60℃ for 10 h. After cooling down to room temperature, the product was washed three times with ethanol, and finally dried in a vacuum drying oven at 60℃ for 12 h to obtain Ni-ZIF.

Preparation of D-Ni-ZIF nanosheet array:

Ni-ZIF (20 mg) was dispersed in KOH ethanol solutions (10 mL, 0.35 M) for 12 h. After the reaction, the solid was washed with ethanol several times, and finally dried in a vacuum drying oven at 60℃ for 12 h to obtain D-Ni-ZIF.

***Characterizations*:**

The powder X-ray diffraction (XRD) patterns were recorded on a SmartLab. X-ray photoelectron spectroscopy (XPS) measurements were performed on an ESCALAB 250Xi. The N_2 adsorption and desorption measurements were measured on a Micrometitics surface area analyzer (ASAP 2460). The morphology of the samples was investigated using scanning electron microscope (SEM S-4800) with an accelerating voltage of 20 kV, combined with energy dispersive X-ray spectroscopy (EDX) for the elemental analysis. Transmission electron microscopic (TEM) and high-resolution TEM (HRTEM) was recorded on a JEOL JEM-2100 with an accelerating voltage of 200 kV. Details of morphology and EDX mapping were performed on a JEM-2100F at 200 kV.

***Electrochemical measurements*:**

All tests on OER and MOR were operated in a standard three-electrode glass cell by a CHI 660E electrochemistry workstation. The Ni-ZIF, Ag NWs, Ag NWs-Ni-ZIF and D-Ag NWs-Ni-ZIF were directly used as the working electrode (mass of 1 $mg \cdot cm^{-2}$), the reference and counter electrodes were Hg/HgO (1.0 M KOH) electrode and Pt plate, respectively. The electrolyte for OER testing was in 1 M KOH aqueous solution

and was continuously filled with high-purity N_2 gas flow, and additional methanol solution for MOR test electrolyte. The linear sweep voltammetry (LSV) curve was recorded at a scan rate of 5 $mV \cdot s^{-1}$. The electrochemical impedance spectroscopy (EIS) was measured over a frequency range from 0.01 to 100000 Hz. All potentials are referenced to the Hg/HgO (1M KOH) reference electrode. The measured potentials relative to Hg/HgO can be converted to the reversible hydrogen electrode (RHE) using the following formula:

$$E_{vs\ RHE} = E_{vs\ Hg/HgO} + 0.0982 + 0.0592pH.$$

The ECSA value for the synthesized catalysts was calculated by the following equation:

$$ECSA=Cdl / Cs$$

where Cs represents a general specific capacitance of 0.04 mF cm^{-2} on the basis of a typical value reported for metal electrodes in alkaline solution.

The relevant electrochemical calculations

Tafel slope: The Tafel slope was examined by the corresponding LSVs according to the equation:

$\eta = b \bullet \log J + a$

where η, b, J, and a represent the overpotential, Tafel slope, current density, the overpotential at 1 $mA \cdot cm^{-2}$, respectively.

***Electrochemically active surface area (ECSA) calculation*:**

ECSA is proportional to the double layer capacitance (C_{dl}) and can be evaluated by capacitance measurement. The C_{dl} can be measured from cyclic voltammetry (*CV*) in a non-Faradaic region of 1.127-1.217 V versus (*vs*.) reversible hydrogen electrode (RHE) at scan rates of 5, 10, 20, 30, 50 and 70 mV s^{-1} , respectively.

Methanol conversion and product quantification

The electrochemical oxidation of methanol was carried out at room temperature with stirring by chronoamperometry (i-t) at 1.717 V (vs RHE) for 0-20 hours.

The identification of molecular structure of formate in the anode product is conducted by Nuclear magnetic resonance (NMR) spectroscopy were recorded on JNM-ECZ600R instruments at 600 MHz (^{1}H NMR) and 150 MHz (^{13}C NMR). All the NMR spectra were measured in D_2O.

The identification and quantification of formate product are conducted by Ion Chromatography (IC) and determined by calibration curve. The anode solution was then proportionately (100 fold) diluted and analyzed by Ion Chromatography (IC) to detect the formate generation. The Ion Chromatography (IC) was carried out on a ICS-3000 ion chromatograph (Shenghan Chromatography Technology Co., Ltd, Qingdao, China) equipped with an AS-11 column.

The identification and quantification of the formate products were determined by calibration curve by applying standard formate solutions with known concentrations of commercially purchased pure sodium formate (chromatographic pure).

The Faradaic efficiency (FE) of formate generation was calculated using the following equation:

$$FE(formate, \%) = \frac{mole\ of\ formed\ formate}{total\ charge\ passed/(4 \times F)} \times 100\%$$

.

Additional Figures and Tables

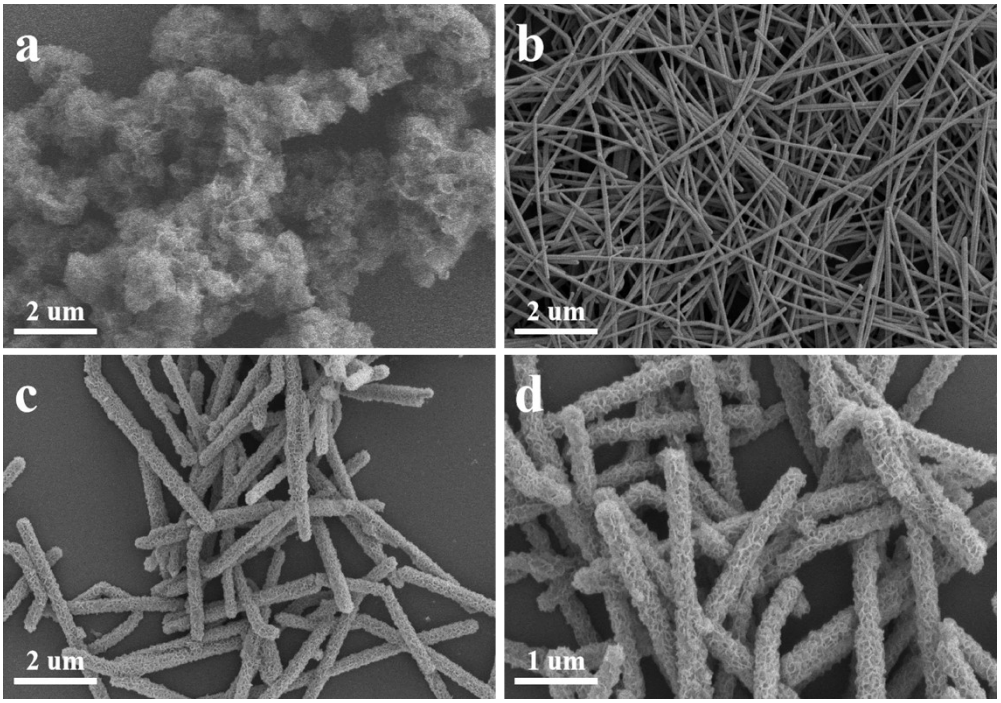

Figure S1. **SEM images of (a) Ni-ZIF, (b) Ag NWs, (c) Ag NWs-Ni-ZIF, and (d) D-Ag NWs-Ni-ZIF.**

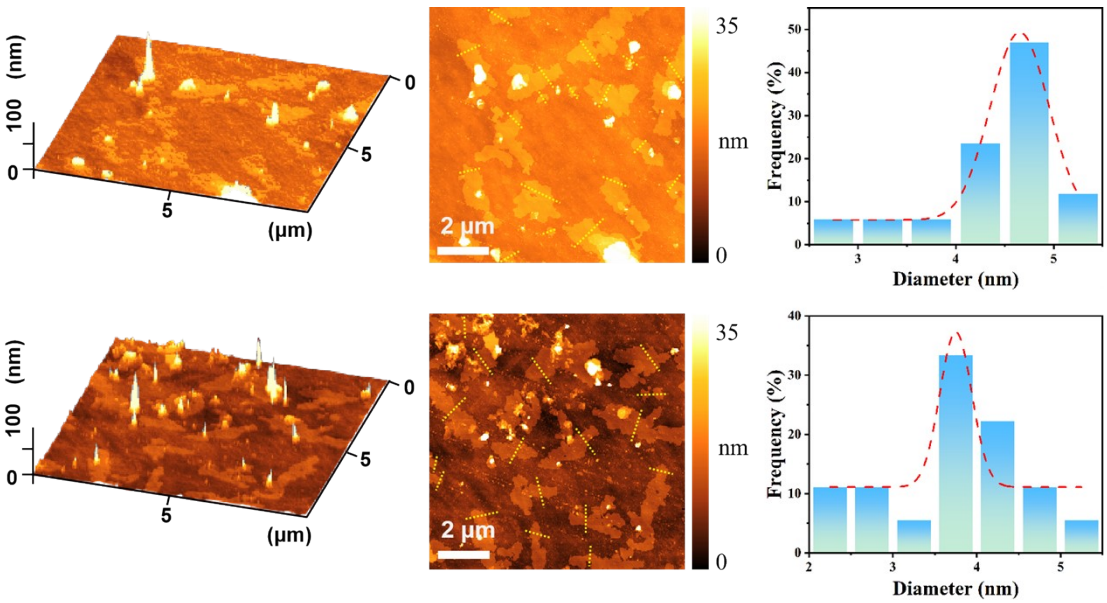

Figure S2. AFM image and Average thickness of nanosheets.

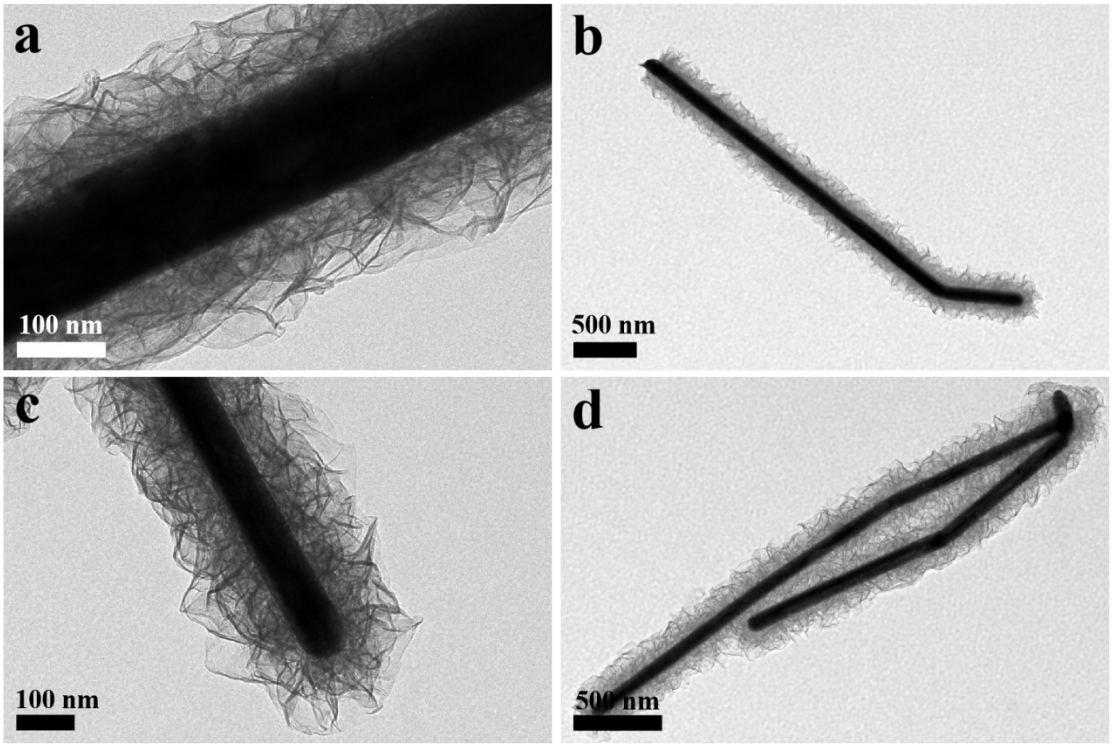

Figure S3. TEM images of (a, b) Ag NWs-Ni-ZIF and (c, d) D-Ag NWs-Ni-ZIF.

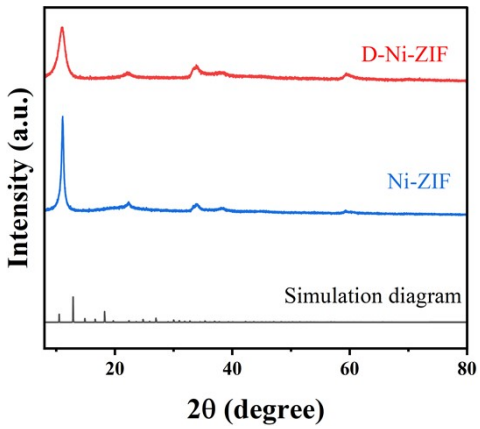

Figure S4. PXRD patterns of Ag NWs-Ni-ZIF and D-Ag NWs-Ni-ZIF as well as simulated patterns.

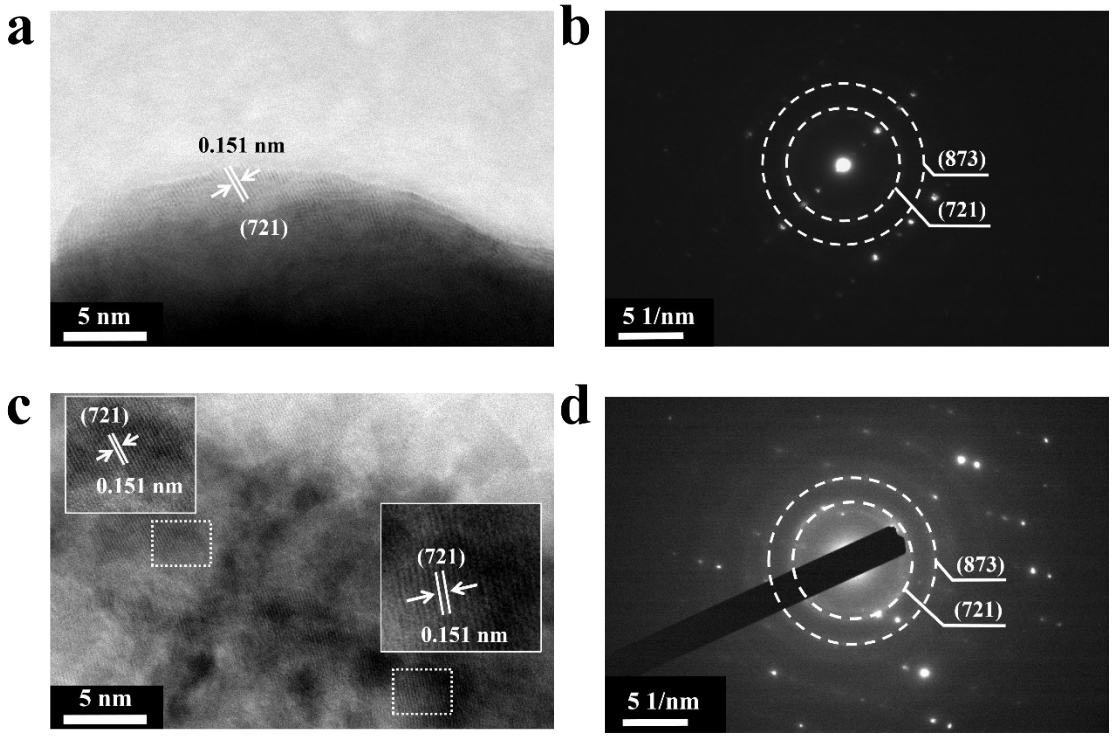

Figure S5. HRTEM images and selective area electron diffraction of Ag NWs-Ni-ZIF (a-b) and D-Ag NWs-Ni-ZIF (c-d), respectively.

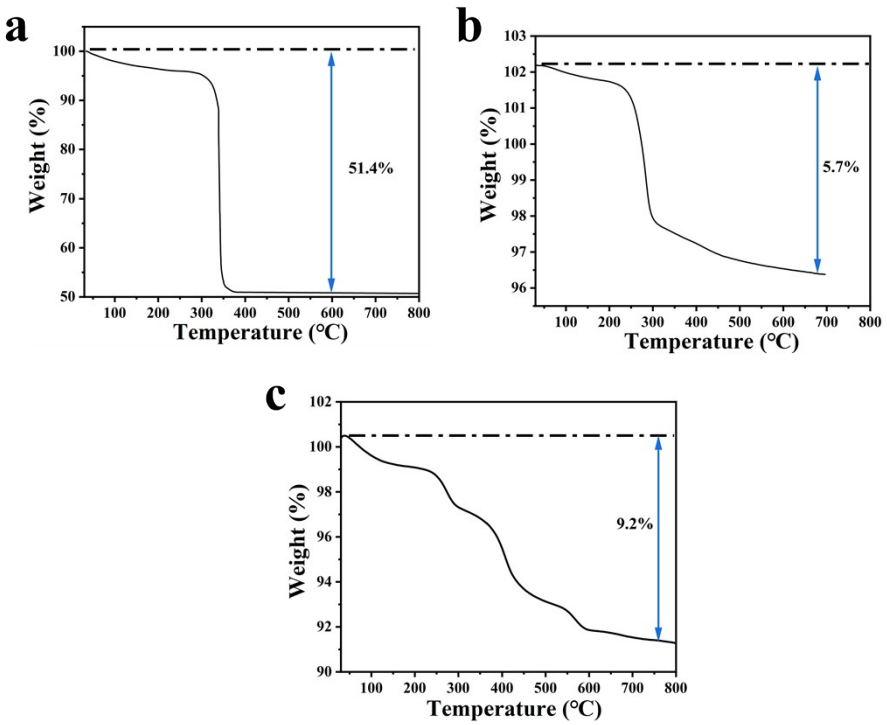

Figure S6. (a) TGA curve of Ni-ZIF, (b) TGA curve of Ag NWs-Ni-ZIF, (c) TGA curve of D-Ag NWs-Ni-ZIF.

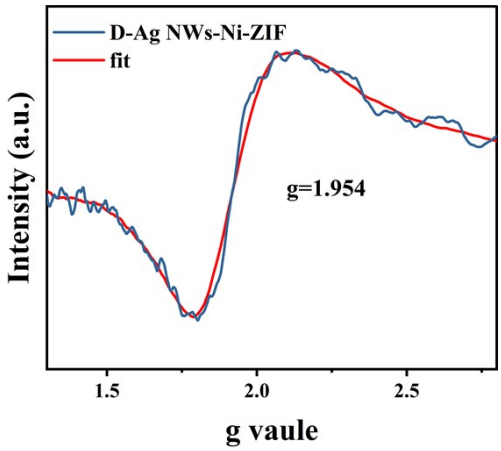

Figure S7. EPR spectrum of D-Ag NWs-Ni-ZIF.

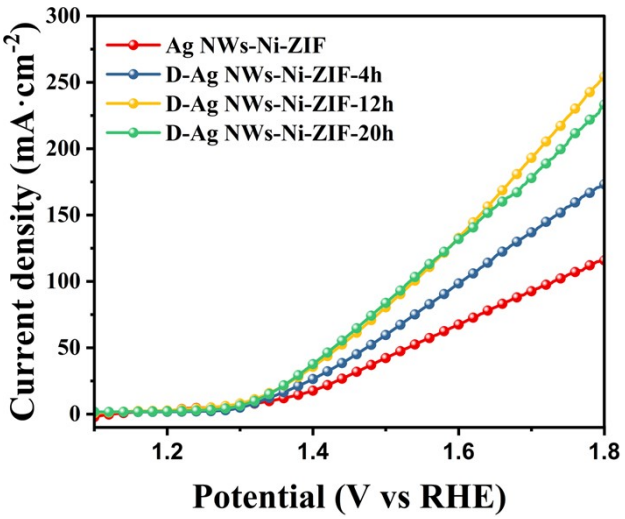

Figure S8. LSV curves of Ag NWs-Ni-ZIF, D-Ag NWs-Ni-ZIF-4h, D-Ag NWs-Ni-ZIF-12h, D-Ag NWs-Ni-ZIF-20h.

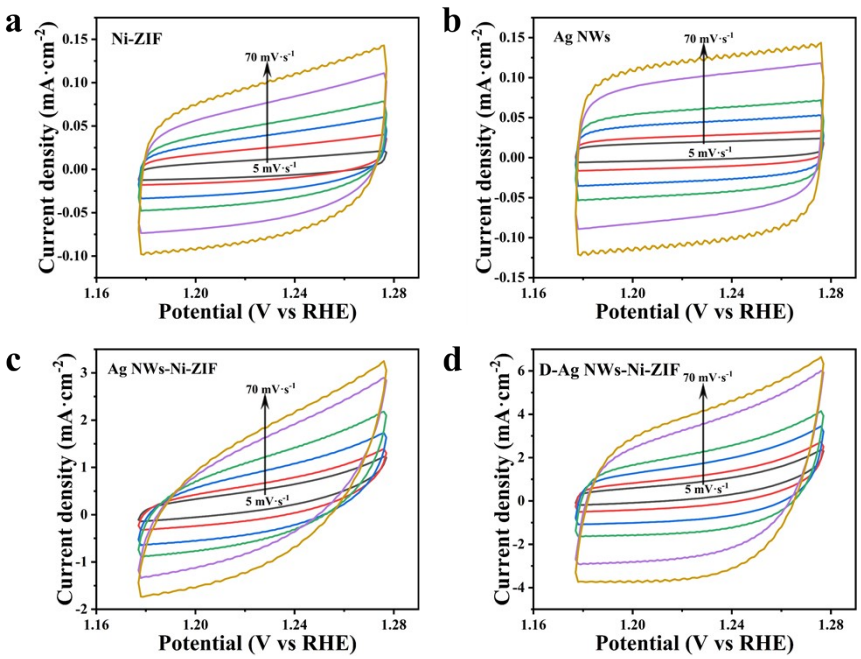

Figure S9. CV curves at different scan rates: (a) Ag NWs, (b) Ni-ZIF, (c) Ag NWs-Ni-ZIF and (d) D-Ag NWs-Ni-ZIF. double layer capacitance (C_{dl}).

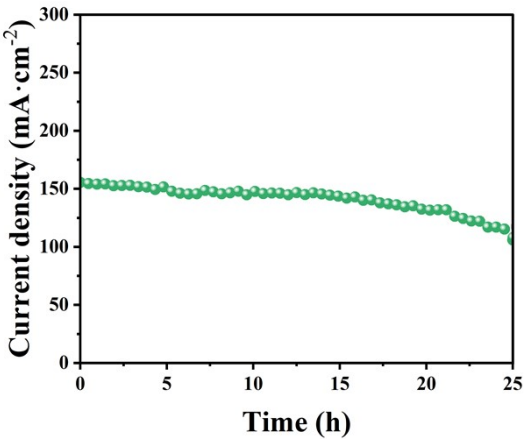

Figure S10. I-t curve of D-Ag NWs-Ni-ZIF at 1.717 V (vs. RHE) potential.

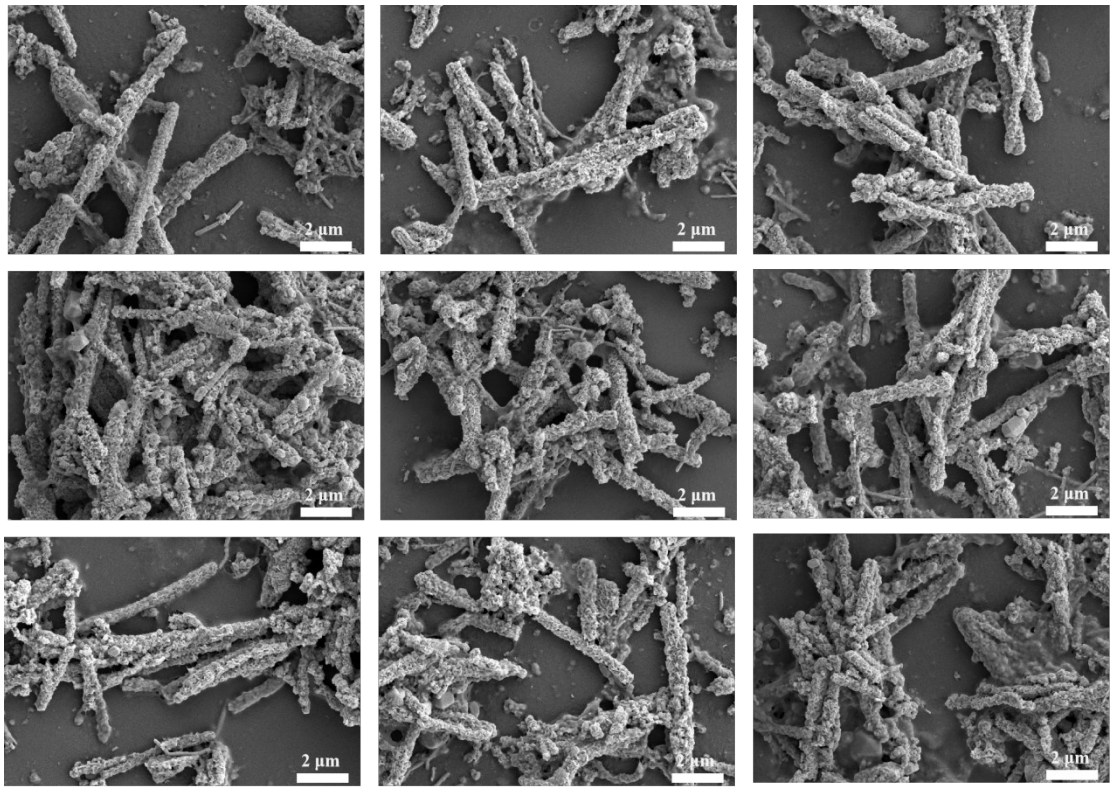

Figure S11. SEM images of D-Ag NWs-Ni-ZIF after electrochemical stability testing.

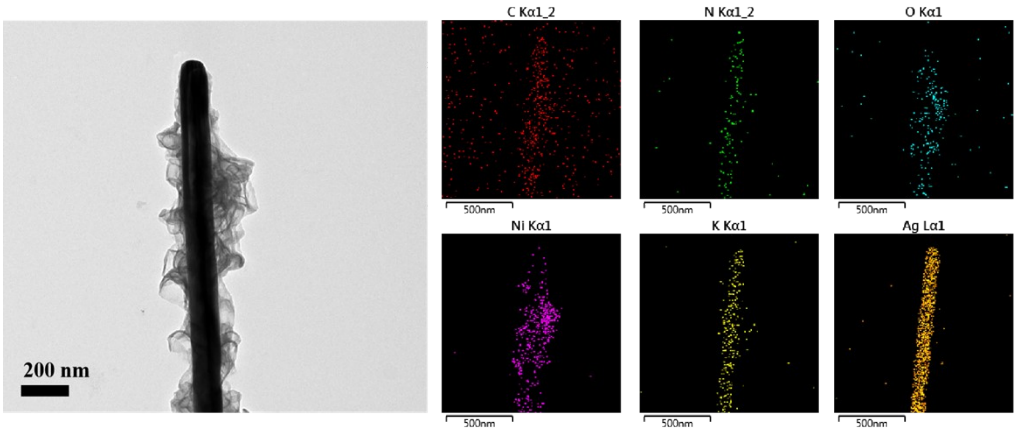

Figure S12. TEM images and Mapping of D-Ag NWs-Ni-ZIF after electrochemical stability testi

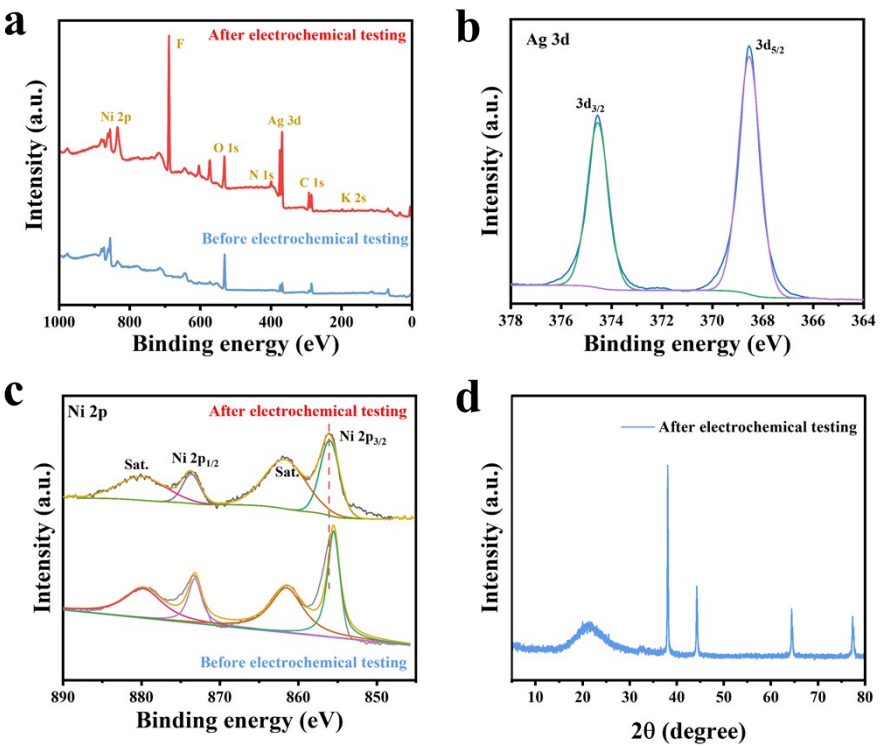

Figure S13. XPS spectra of Ag NWs-Ni-ZIF and D-Ag NWs-Ni-ZIF: (a) Full spectra; (b) Ag 3d high-resolution XPS spectra; (c) Ni 2p high-resolution XPS spectrum. (d) XRD.

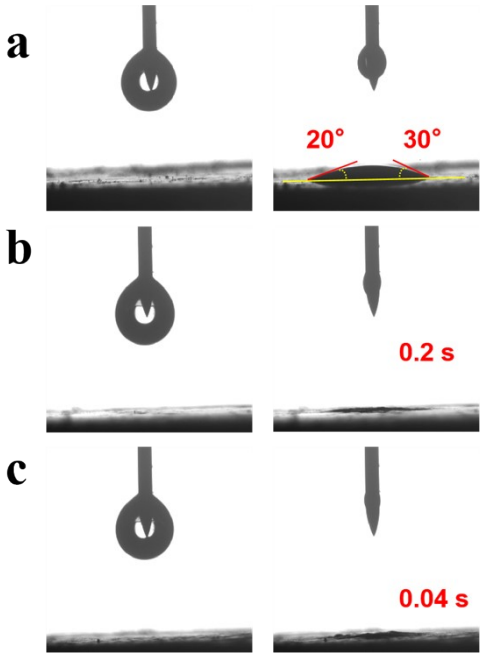

Figure S14. Contact angle test, (a) Ni-ZIF, (b) Ag NWs-Ni-ZIF and (b) D-Ag NWs-Ni-ZIF.

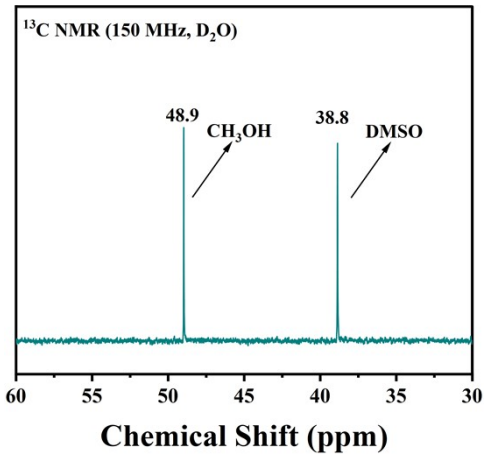

Figure S15. ^{13}C NMR spectra CH_3OH and DMSO.

	Ag (μg/mL)	Ni (μg/mL)	K (μg/mL)
Before electrochemical testing	8.9030	0.7959	0.1491
After electrochemical testing	7.7400	0.4990	0.1115

Table S1. ICP test results of D-Ag NWs-Ni-ZIF. Weigh a certain amount of the sample, digest it with concentrated nitric acid using a microwave, and dilute to 100 mL to make its concentration 10 μg/mL.

Electrocatalysts	Electrolyte	Potential (V vs RHE) at 10 mA·cm^{-2}	ECSA (cm^2)	Reference
D-Ag NWs-Ni-ZIF	1 M KOH+1 M MeOH	1.313	2625	This work
h-NiSe/CNTs/CC	1 M KOH+1 M MeOH	1.370	Unspecified	[1]
CuCo-UMOFNs	1 M KOH+1 M MeOH	1.365	Unspecified	[2]
3D porous Ni networks	1.0 M NaOH + 1.0 M MeOH	1.455	Unspecified	[3]
NiFe NPs	1.0 M NaOH + 1.0 M MeOH	1.541	Unspecified	[4]
Ni_3C/Ni_3S_2	1 M KOH+1 M MeOH	1.37	Unspecified	[5]
$NiCo_2S_4$-MoS_2	1 M KOH+1 M MeOH	1.282	547.25	[6]
Ni/Ni_3S_2-MoO_2@CC	1 M KOH+1 M MeOH	1.370	267.0	[7]
Ni-CeO_2@CN-600	1 M KOH+1 M MeOH	1.361	381.8	[8]
NiSnPH@OOH/CC	1 M KOH+1 M MeOH	1.350	Unspecified	[9]
$Ni_{50}Co_{50}$-m	1 M KOH+1 M MeOH	1.330	0.2460	[10]
Ni-$CuCoN_{0.6}$@CC	1 M KOH+1 M MeOH	1.334	517.50	[11]
Ni film	0.1 M KOH+0.1 M MeOH	1.670	Unspecified	[12]
NixCo1- x$(OH)_2$	1 M KOH+0.5 M MeOH	1.32	Unspecified	[13]
CeO_2-$Ni_{0.85}$Se-550-NC	1 M KOH+0.5 M MeOH	1.309	278.25	[14]
$Co(OH)_2$@HOS/CP	1 M KOH+3 M MeOH	1.385	Unspecified	[15]
NiMn-LDH/NF	1 M KOH + 3 M MeOH	1.33	Unspecified	[16]

Table S2. Comparison of MOR activities for D-Ag NWs-Ni-ZIF and recently reported highly active materials in mixed solvent of 1M KOH and 1 M methanol.

Reference

[1] B. Zhao, J. Liu, C. Xu, R. Feng, P. Sui, L. Wang, J. Zhang, J. L. Luo, X. Z. Fu, *Advanced Functional Materials* 2020, 31.

[2] X. Wei, S. Wang, Z. Hua, L. Chen, J. Shi, *ACS Appl Mater Interfaces* 2018, 10, 25422.

[3] X. Guo, T. Liang, D. Zhang, M. Zhang, Y. Lin, C. Lai, Materials Chemistry and Physics 2019, 221, 390.

[4] S. L. Candelaria, N. M. Bedford, T. J. Woehl, N. S. Rentz, A. R. Showalter, S. Pylypenko, B. A. Bunker, S. Lee, B. Reinhart, Y. Ren, S. P. Ertem, E. B. Coughlin, N. A. Sather, J. L. Horan, A. M. Herring, L. F. Greenlee, ACS Catalysis 2016, 7, 365.

[5] JGL Tao, J Chen, B Zhao, R Feng, M Shakouri and F Chen, Small, 2024, 20, 2402492.

[6] F Jia, Y Zhang, X Ma, Z Zheng, F An and T Hu, J. Colloid Interface Sci., 2025, 693: 137650.

[7] F. Jia, Y. Zhang, P. Zhang, X. Zhang, T. Hu, Appl. Surf. Sci., 2023, 640, 158348-158356.

[8] J. Linghu, R. Guo, Y. Zhang, X. Zhang, T. Hu, Appl. Surf. Sci., 2023,631, 157499-157507.

[19] J. Shao, Y. Fang, X. Wu, M.I. Abdullah, Y. Tao, Nano Res., 2024, 17, 2388–2399.

[10] Y. Qi, Y. Zhu, H. Jiang, C. Li, Chinese J. Catal., 2024,56, 139-149.

[11] F. Jia, Y. Zhang, X. Zhang, T. Hu, J. Colloid Interf. Sci.,2025, 677, 597-607.

[12] D. Chen, S. D. Minteer, Journal of Power Sources 2015, 284, 27.

[13] L. Mei, D. Xiaohui, X. Kun, L. Yue, Z. Bin, H. Jie, L. Jing-Li, F. Xian-Zhu, ChemSusChem 2020, 13.

[14] T Yue, Y Shi, Y Ji, J Jia, Y Chang, J Chen and M Jia, J. Colloid Interface Sci. 2024, 653, 1369-1378.

[15] K. Xiang, D. Wu, X. Deng, M. Li, S. Chen, P. Hao, X. Guo, J. L. Luo, X. Z. Fu, Advanced Functional Materials 2020, 30.

[16] B Zhu, B Dong, F Wang, Q Yang, Y He, C Zhang, P Jin and L Feng, Nat. Commun. 2023, 11, 1686.